Shubbar, AAF, Jafer, H, Abdulredha, M, Al-Khafaji, ZS, Nasr, MS, Al Masoodi, Z and Sadique, MM

Properties of cement mortar incorporated high volume fraction of GGBFS and CKD from 1 day to 550 days

Properties of cement mortar incorporated high volume fraction of GGBFS and CKD from 1 day to 550 days

Ali Abdulhussein Shubbar [a, b *], Hassnen Jafer [b], Muhammad Abdulredha [c], Zainab S. Al-Khafaji [d], Mohammed Salah Nasr [e], Zainab Al Masoodi [f], Monower Sadique [a]

[a] Department of Civil Engineering, Liverpool John Moores University, Henry Cotton Building, Webster Street, Liverpool L3 2ET, UK.

[b] Department of Civil Engineering, College of Engineering, University of Babylon, Babylon, Iraq

[c] Department of Civil Engineering, College of Engineering, University of Kerbala, Kerbala, Iraq

[d] Department of Civil Engineering, Al- Mustaqbal University College, Babylon, Iraq

[e] Babylon Technical Institute, Al-Furat Al-Awsat Technical University, 51015 Babylon, Iraq.

[f] Department of Civil Engineering, College of Engineering, University of Warith Alanbiyaa, Kerbala, Iraq

* Corresponding author:

A.A.SHUBBAR@2014.LJMU.AC.UK, alishubbar993@gmail.com (A.A.Shubbar)

Abstract

This study aims to investigate the effect of cement replacement with high volume fraction of ground granulated blast furnace slag (GGBFS) and cement kiln dust (CKD) on mechanical, durability and microstructural properties of cement mortar from 1day to 550 days. Compressive strength and ultrasonic pulse velocity (UPV) were used to evaluate the mortars' performance. Besides, statistical analyses were conducted to predict mortars' mechanical and durability performance as well as investigate the influence of mortars' properties (mixture and curing time) on their performance. The results indicated that replacing the cement with up to 60% GGBFS and CKD showed a comparable behavior to the cement after 28 days of curing onward. The statistical analysis revealed that the developed models achieved high level of agreement between the predicted and observed results with a coefficient of determination (R^2) of more than 0.97. The findings in this study announced on the development of promising binder that can be used in different construction sectors with the benefits of reducing the CO_2 emissions.

Keywords: Compressive strength; cement kiln dust; early and later ages; high volume fraction; ground granulated blast furnace slag; multiple regression.

1. Introduction

At the beginning of the twenty-first century, about a hundred and eighty-nine countries around the world were adopting the Declaration of United Nation Millennium creating Millennium Development Goals (MDGs) when they decided to work together for the new generation future [1]. MDGs set an ambitious list of goals to increase worldwide progress on social development, economic development and sustainability of environment [1]. Sustainability in the construction industry focuses on the materials selection, preparation and durability, ongoing efforts to produce a new sustainable solutions to replace well-known materials fully or partially.

Global warming related directly to the Greenhouse Gasses (GHGs) phenomena considered as one of the main risks humanity facing nowadays as a result of its detrimental impact on the planet [2]. CO_2 emissions are among the gasses that contributing considerably to GHGs [3]. Cement is the most important building material that has been used worldwide as a binder (glue) in numerous construction activities like bridges, buildings, roads, etc. [4, 5]. However, the cement usage has many financial and environmental disadvantages. Van Ruijven et al., [6] indicated that cement production is an intensive power consumer sector with about 15% of the worldwide industrial power consumption following steel sector. It is also estimated that the production of one tonne of cement requires nearly 1500 kg of quarry material, leading to the production of roughly 1000 kg of CO_2 emissions [7, 8].

Cement manufacturing has therefore become one of the world's main issues and it is very important to transform the building materials sector towards sustainable production by seeking alternative resources to substitute or decrease the use of cement. Consequently, the search for alternative products, like waste or/and by-product products that are usually referred to as supplementary cementitious products (SCMs), to be utilised as cement substitute in the construction field could be an important effort as a sustainable solution to reduce the production

of cement and GHGs, in order to achieve an environmentally friendly sector. These materials have a main role in meeting the objective of achieving sustainable construction materials.

Large amounts of SCMs are produced daily from various industries around the world. Also, they have a harmful impact on the environment and sustainable resources owing to the possibility of contaminations depletion to the soil and groundwater (if heavy metals are discovered in their chemical composition) as well as the cost of disposal [4, 9]. Consequently, the reuse of SCMs from variant resources could therefore be useful in terms of sustainability and could be utilised as cement substitutes that contribute to the decrease of GHGs and the price of building products by offering similar efficiency to that of conventional cement [9, 10].

Several studies were conducted utilising SCMs to substitute a part of the cement in binders for use in various building industries like concrete building, rigid pavements and stabilizing the soft soil [11-13]. The use of these products in the cement sector has increased the advantages by decreasing the clinker quantity, which in turn decreases the adverse environmental impact of cement and could improve several characteristics of cement [10].

The composition of SCMs contain several minerals, where some SCMs contain calcium with high to moderate components such as ground granulated blast furnace slag (GGBFS) and cement kiln dust (CKD) in their chemical composition. These products have the characteristic of self-cementing at varying concentrations depending on the availability of free lime in their chemical compositions [14, 15]. When such materials activated with other products like cement, lime and (other kinds of fly ashes as pozzolanic activators) these materials can play a good role in the process of hydration [14, 16].

In many researches, GGBFS has been used as a cement substitute to create fresh low-carbon binders. Roughly, all investigations indicated that GGBFS could be a precious substitute for cement with binder efficiency similar to cement performance alone. Nevertheless, it has been

observed that GGBFS needs activation with other chemical components like alkaline materials to enhance its efficiency as stated by Karthik et al. [17] and Sargent et al. [18]. Generally speaking, GGBFS has two phases: the first phase which is in charge of the GGBFS hydration called as the crystalline phase, while the second phase is called glassy phase, which is responsible for the GGBFS cementitious properties [19]. Compared to cement, many researchers have found that GGBFS has many benefits, like enhancing the bond between particles, thereby decreasing concrete permeability and improving durability [20, 21]. However, due to the aforementioned advantages of utilizing GGBFS in the construction industry, it is expected that the price of GGBFS will be increased.

There is therefore a need for various, inexpensive waste products that can be utilised in addition to GGBFS to partly substitute conventional cement. This waste material could be cement kiln dust (CKD), a waste material generated during the process of cement manufacturing. CKD is an extremely alkaline, fine-grained by-product material that presents around 3% to 4% of the complete cement generated during the manufacture of cement and has a chemical compositions comparable to that of conventional cement [22]. CKD is classified as a safe (non-hazardous) solid waste materials according to The Agency of Environmental Protection [23]. The CKD is normally rich with compositions of alkaline like Na_2O and K_2O [23]. Additionally, the CKD has extremely high pH value (around 12) and that could be responsible for the natural alkaline activator to GGBFS [24, 25].

Ternary mixed binder manufacturing could considerably enhance concrete efficiency compared to conventional Ordinary Portland cement (OPC) or binary mixed cements (OPC-GGBFS cements). This is attributed to the mixing procedure where homogeneous nucleation may occur between various particle sized fractions leading to the development of a dense microstructure of hardened product with enhanced durability [26, 27].

Additionally, scholars have shown a particular interest in the development of statistical models for experimental research as it significantly helps researchers to optimise, reproduce or redesign their experiments [28-30]. For example, Jafer et al. [31] used statistical modelling to investigate the influence of several experimental parameters on the strength of stabilised soil, while Alattabi et al. [32] employed multiple linear regression to predict the performance of two-stage settling sequencing batch reactor based on the parameters of the treated wastewater. Statistical modelling also helps to view the causes and the effects for any experiment from multiple perspectives to identify potential consequences and implement changes to reduce defects or errors [33]. Thus, a part of this research has been devoted to building numerical models that assess the influence of the curing time and mixture on the mechanical and durability performance of the developed mortars.

Limited studies were considered evaluating the performance of cement mortars incorporating high volume fraction of supplementary cementitious materials at both early and later ages (beyond one year). Therefore, the novelty of this research is utilizing and evaluating the performance of GGBS/CKD combinations as supplementary cementitious materials at high volume fractions in cement mortar from 1 day to 550 days. Accordingly, this research aims firstly to prepare a cheap and eco-friendly binder with a high volume fraction of SCMs by partial substitution of OPC with a mixture of GGBS and CKD. To achieve this aim, mortar mixtures were made and their mechanical, durability and microstructural characteristics were evaluated from 1 day to 550 days. The other aim of this research is to build numerical models that assess the influence of the curing time and mixture on the mechanical and durability performance of the developed mortars.

2. Research Significance

The rise in global population has resulted in an increase in demand for the use of construction materials, mainly cement. The cement industry emits significant amounts of greenhouse gases and contributes towards global warming. In addition, the cement industry depletes natural resources and affects the development of sustainability. This study aims to reduce this environmentally harmful effect through decreasing the cement content in the mixture by partially replacing it with a high volume fraction of industrial wastes/by-products (GGBS/CKD combinations). The results obtained in this study are promising as cement content can be reduced by 60% without affecting its different properties.

3. Materials and Methodology

3.1. Materials

3.1.1 Sand

In this project, the sand was passed through a 3.35mm IS sieve. The sand has a particle size distribution as demonstrated in Fig. 1 with a specific gravity of 2.62.

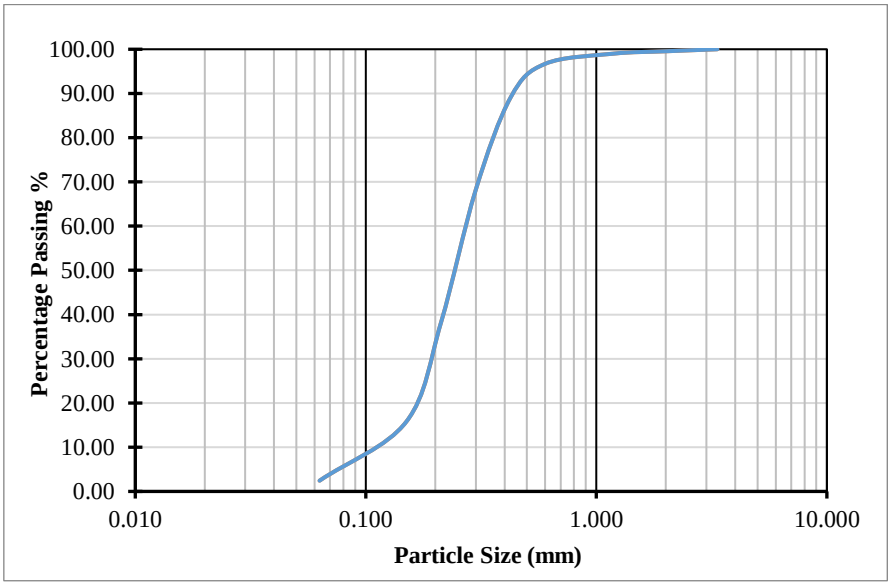

Fig. 1: The sand's Particle size distribution.

155 ***3.1.2 Water***

156 Normal tap water was utilised for mixing and curing of samples.

157 ***3.1.3 Binder Materials***

158 In this research, three materials have been utilised in ternary blended binder production. The
159 materials were Ordinary Portland Cement (OPC), Cement Kiln Dust (CKD) and Ground
160 Granulated Blast Furnace Slag (GGBFS). The cement utilized during the research was OPC
161 kind CEM-II / A / LL 32.5-N that conforms to the BS EN 197-1 [34]. CEMEX Quality
162 Department, Warwickshire, UK supplied the OPC and CKD while Hanson Heidelberg Cement
163 Group, Scunthorpe, UK supplied the GGBFS.

164 So as to identify the Particle Size Distribution (PSD) of the OPC, GGBFS and CKD, a Beckman
165 Coulter laser particle size analyser was utilised. Additionally, the specific surface area (SSA)
166 of the OPC, GGBFS and CKD was also measured utilizing Blaine air-permeability apparatus.
167 The curves of PSD for the OPC, GGBFS and CKD are presented in Fig. 2 as gained from the
168 laser particle size analyser. Table 1 demonstrates the variances in d_{50}, the SSA and the specific
169 gravity of the OPC, GGBFS and CKD.

170 Table 1: The variances in d_{50}, SSA and specific gravity of the binder materials.

Detail	**OPC**	**GGBFS**	**CKD**
d_{50} (μm)	12.660	7.523	26.95
SSA (cm^2/g)	4296	6931	3566
Specific gravity	2.936	3.05	2.983

171

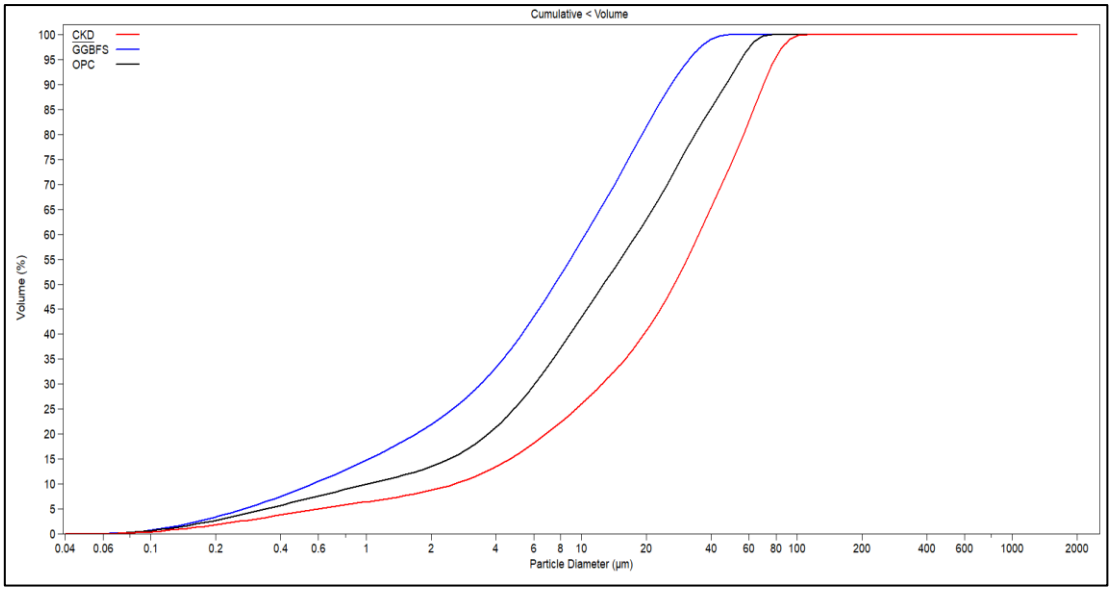

Fig. 2: The accumulative distribution of particle size for OPC, CKD and GGBFS.

The PSD and SSA of the binder materials have a considerable effect on the mortar's compressive strength. It has been stated by Celik et al. [35] that higher strength of concrete was obtained for concrete made with finer SCMs as partial substitute to cement. Fig. 2 and Table 1 clearly shows that the finest particles were GGBFS particles in comparison with the other binder materials. On the other hand, the largest particles were CKD particles relative to OPC, and that could retard the mortars' performance during hydration reactivity [36, 37].

The binder materials (OPC, CKD and GGBFS) were chemically analysed utilizing Shimadzu EDX-720 an Energy Dispersive X-ray Florescence Spectrometer (EDXRF). The chemical compositions of the binder materials (OPC, CKD and GGBFS) are obtainable in Table 2. It could be observed from Table 2 that GGBFS has high proportions of CaO and SiO_2 while the CKD has higher proportion of CaO relative to GGBFS. Additionally, the CKD has higher alkali (K_2O %) and sulphates (SO_3%) relative to OPC.

186 Table 2: Chemical analysis for OPC, HCFA and GGBFS.

Detail	OPC	GGBFS	CKD
CaO %	65.21	42.51	57.23
Al_2O_3 %	1.70	5.12	4.2
Fe_2O_3 %	1.64	-	3.8
SiO_2 %	24.56	41.06	16.52
MgO %	1.30	4.25	0.8
Na_2O %	1.34	3.09	0.23
K_2O %	0.82	0.69	6.72
SO_3 %	2.62	1.27	4.31
pH	12.73	11.02	12.75

187

188 Fig. 3 shows the Scanning Electron Microscopy (SEM) images of the candidate materials used
189 to produce the new binder in their powder un-hydrated state. The SEM testing of the powder
190 material revealed that the particle shape of both OPC and GGBFS is irregular and angular while
191 the particles of CKD are coagulated and agglomerated as shown in Fig. 3.

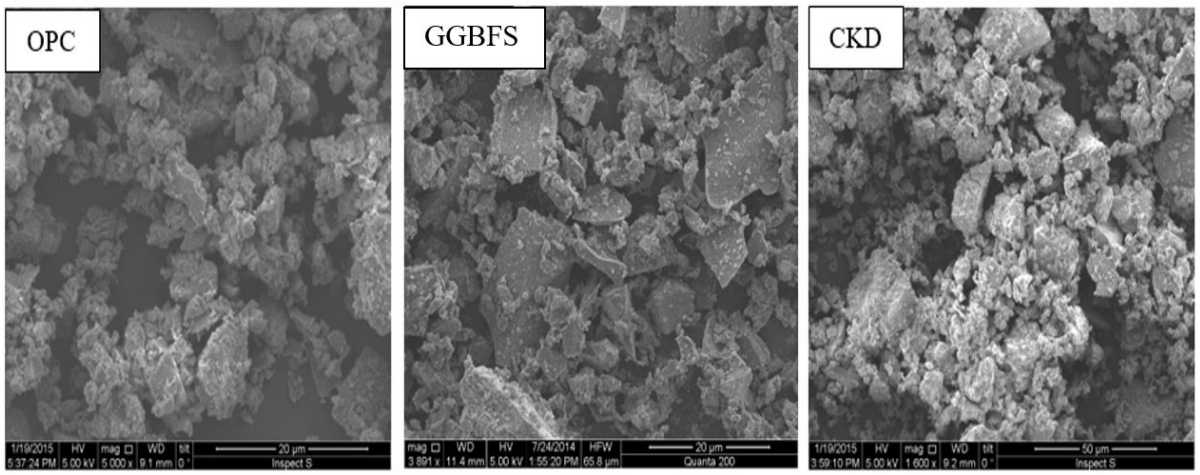

192

193 Fig. 3. SEM images of the candidate materials used in the study.

3.2 Mixing Proportions

Dhir et al. [38] replaced the cement by a constant percentage (35% of the total binder) of GGBS/CKD combinations. Five blends were made in which the GGBS to CKD ratios were varied from 0 to 100%. They concluded that the optimum performance was achieved at a GGBS/CKD ratio of 3 and the difference in the compressive strength in comparison with samples made with GGBS/CKD ratio of 2 was negligible. Therefore, in this study the GGBS/CKD ratio was chosen as 2 in order to increase the usage of CKD in the mixture, thus improving the environmental and economic performance of the new developed binder. The GGBFS and CKD were initially blended to prepare binary blended binder material (BBBM), then the BBBM was utilised to partially replace OPC to produce ternary blended binders. Table 3 shows the ratios of mixing for the ternary blending mixes. During this research, the ratios of water/binder (W/B) and sand/binder (S/B) were fixed as 0.4 and 2.5, respectively.

Table 3: Mix proportion details of the mortar prepared with different proportions of OPC, GGBFS and CKD.

Mix ID	OPC (g)	GGBFS (g)	CKD (g)	Sand (g)	Water (g)
REF	150	0	0	375	60
T20	120	20	10	375	60
T40	90	40	20	375	60
T60	60	60	30	375	60
T80	30	80	40	375	60

The equivalent alkalinity ($Na_2O + 0.658\ K_2O$) of T20, T40, T60 and T80 mixtures were 2.29, 2.69, 3.10 and 3.51% respectively. It was evident that these percentages have exceeded the limits ($Na_2O + 0.658\ K_2O \leq 0.6\%$) specified by the international standards for OPC to prevent the potential damage caused by alkali-silica reactivity (ASR). However, according to Hester et al. [39], up to 50% substitution of cement with GGBFS, the GGBFS concretes had very low expansion levels (at equivalent alkalinity loads of 5 and 6 kg/m3). They attributed that reduction to that, at high substitution levels, the GGBFS suppressed the transport of hydroxyl ions (OH) to such an extent that it counteracted the potential adverse effect of the increased alkalinity. Therefore, this is another reason of mixing the GGBFS with CKD at GGBFS/CKD ratio of 2 in this research to overcome such a problem.

3.3 Testing Programme

3.3.1 Setting time and Standard consistency

The fresh characteristics (setting time and standard consistency) of the ternary paste mixtures were tested utilizing the Vicat apparatus in accordance with BS EN 196-3 [40]

3.3.2 Compressive strength

Compression testing was conducted by a compression machine brand Control Automax 5 according to BS EN 196-1 [41]. This apparatus features a precise load rate implementation and the data of the failure can be acquired and downloaded to a machine-connected computer. The data is displayed directly in both stresses and loads. Specimens of every ternary mixes were tested after subjecting to various curing phases; 1, 2, 3, 7, 14, 21, 28, 56, 90 and 550 day except the samples for mixture T20 that were cured until the age of 28 days. Two specimens with dimensions of 40x40x160 mm were produced for every blending ratio at every curing period. Each specimen was broken into two part by three points loading of the prism specimens and an average of four parts were taken to represent the final compressive strength values.

3.3.3 Test of Ultrasonic Pulse Velocity (UPV)

This test is one of the non-distractive tests used to assess the durability of mortar and/or concrete specimens [42]. A Proceq ultrasonic pulse machine was utilised to determine the transit time required for ultrasonic waves to travel from the transducer and receive the transducer through the interposed mortar specimens in accordance with BS 1881-203: 1986 [43]. For this purpose, four cubic specimens that have dimensions of 100X100X100 mm were prepared and subjected to similar curing periods as compressive strength testing (1, 2, 3, 7, 14, 21, 28, 56, 90 and 550 day) except the samples for mixture T20 that were cured until the age of 28 days. The results of this experiment could be useful to offer an indication of durability by evaluating the reduction of the voids through the healing moment as the velocity rises with the decrease of the voids inside the tested specimen owing to the rise in density resulting in a compact and denser structure.

3.3.4 Scanning Electron Microscopy (SEM) and Energy Dispersive X-ray Spectroscopy (EDX) Analyses

SEM is the most commonly utilised method for analysing the morphology of hardened products and evaluating the degree of hydration in the cement studies sector [44]. Though SEM is a method that is susceptible to the surface, it could still provide a lot of data about the surface of the specimens that is of particular importance since the surface of the specimen is the first location that will accommodate any reactions [45]. After 1, 3, 7, 28, 90 and 550 days of curing, SEM testing was conducted to assess the morphology of each raw material in its powder state and optimal ternary mixed binder material paste. Additionally, EDX analysis was also performed in this study for the optimal ternary mixed binder material paste after 1, 3, 7 and 28 days to analyse its elemental composition. Both tests were performed utilizing a 5-20 kV accelerating voltage for EDX Oxford Inca x-act sensor, a FEI SEM model Inspect S and a

Quanta 200. The specimens were coated with a gold layer utilizing a sputter coater to increase visibility before the tests were performed.

3.4 Numerical analysis

The experimental results were numerically analysed to investigate the influence of the experimental parameters (curing time and mixture) on the mechanical and durability properties of the mortars, using the SPSS-26 package. The results for the ternary mixture T20 were not included in the numerical analysis due to the shortage in data after the age of 28 days that significantly affect the results of the numerical analysis model. Multiple regression (MR), a family of techniques used to model the relationship between several explanatory variables (EVs) and a response variable (RV) by fitting a linear equation as shown in Equation (1) [30, 33, 46], has been employed in this study. This technique was selected owing to its simple algorithm [30, 47], wide application [46, 48] and achievable validation [33, 49].

$$K = m_0 + \sum_{i=1}^{j} m_i x_i + \varepsilon \quad (1)$$

where K is the predicted RV, m_i are the regression coefficients, x_i are the EVs, j is the number of EVs and ε is a residual error coefficient.

Researchers [50-53] stated that mortars' properties are functions of the experimental parameters e.g. curing time, curing type and materials. In the current study, two models were developed to assess the influence of experimental parameters on the compressive strength and the durability of the mortars. Based on this, to develop reliable MR models, it is essential to meet the assumptions of MR technique [33, 46, 49] namely type of variables, dataset size, normality of continues variables (EVs and RV) collinearity among EVs and presence of outliers in addition to assess the EVs contribution and model's prediction accuracy [54, 55] .

Laerd Statistics [49] stated that RV must be a continuous variable and the EVs should be either continuous or nominal variables in order to employ MR technique for production analysis. In addition, Pallant [46] and Abdulredha et al. [30] indicated that the following equation can be used, taking into account the number of EVs, to determine the minimum required dataset size to build a generalizable MR model:

$$n \geq 50 + 8 * j \quad (2)$$

where n is the size of the experimental dataset and j is the number of EVs.

The production of the developed MR is more robust if the distribution of the continues variables is normal [33, 46]. Normality can be assessed using the Kolmogorov-Smirnov's test [33, 49], where the statistical significance (p) of the latter test must be greater than 0.05 [46]. If otherwise, many transformation methods are available in the literature depending on the direction and the extent of the skewness from the normal distribution e.g. logarithmic transformations [33, 49].

Collinearity of EVs and outlying cases are important assumptions need to be investigated in the preliminary stages of developing MR models [33]. Collinearity refers to the existence of a strong relation between two EVs, which can be solved by excluding one of the related EVs [46, 49]. Collinearity can be identified by calculating the tolerance value for each EV, where a value of 0.1 or less confirms the presence of collinearity in the used dataset [30, 33]. Outliers, on the other hand, are cases with extreme values, which make the outcome of the MR model invalid [49]. Outliers can be spotted by calculating the standardised residuals; any case with a residuals value out the range of ±3.3 must be considered as an outlier and excluded from the analysis if deemed necessary [30, 33, 46].

After checking the MR assumptions have been met, it is essential to assess the contribution of the EVs and the performance of the prediction model [47]. The relative importance of each EV

contribution can be assessed by determining the regression coefficient (m) and statistical significance (p) [46]. The regression coefficient shows the contribution of each EV on the variation in the predicted score of RV. The contribution varies from tangible to negligible according to the statistical significance of each EV [33, 49]. A p-value of less than 0.05 suggests that the EV has a tangible contribution to the developed prediction model [49].

The performance of each developed MR model in explaining the association between the EVs and the RV can be assessed through calculating the coefficient of determination (R2) [30, 33, 47]. The latter coefficient (Equation (3)) shows the concordance between the predicted score of the RV and observed score of the RV, where R2 of 1 or closer to 1 suggests that the model can produce a reliable prediction [46, 49].

$$R^2 = \frac{\sum_{i=1}^{n}(P_i-\bar{Y})^2}{\sum_{i=1}^{n}(O_i-\bar{Y})^2} \quad (3)$$

where $\bar{Y}$ is the mean of the RV, P_i are the predicted scores of the RV, O_i are the observed scores of the RV and n is the size of the experimental dataset.

4. Results and discussion

4.1. Consistency and setting time

Table 4 presents the results of the consistency and initial and final setting times of all the ternary mixtures along with the reference mixture (REF). The standard consistency test depends mainly on the water to binder ratio, rate of hydration reactions and fineness of the binder materials [51]. From Table 4, it can be recognized that the standard consistency (water demand) increased with the increase in the materials replacing OPC to produce T20, T40, T60 and T80. The highest value of consistency was recorded for the mixture T80 which contains the lowest content of cement while T20 indicated a lower consistency among the other ternary mixtures. This behaviour could be attributed to the higher specific surface area of GGBFS relative to

OPC and the high alkalinity, sulphate, volatile salts and free lime content of CKD along with the coarseness, particle size irregularity and high void spaces that all illustrated the high water demand of CKD as can be seen from the SEM image of the CKD in Fig 3 [51, 56-58].

Table 4. Standard consistency and setting times

Mixture ID	Consistency (%)	Initial setting time (min)	Final setting time (min)
REF (100% OPC)	33	270	290
T20	34	271	297
T40	35	275	305
T60	36	285	310
T80	37	290	325

As per the results of setting times shown in Table 4, the results indicated increments in both initial and final setting times of the binder paste after incorporating the replacement materials (GGBFS and CKD). There were gradual increments in the initial setting times with the increase of the GGBFS and CKD content with a higher increase for the ternary mixture T80 (290 minutes which is approximately 7.5% longer than that for REF). A similar behaviour was observed for the final setting time. However, a noticeable increase in the final setting time was found in T80 in comparison to that for the reference cement and T60. This behaviour could be attributed to the reduction occurred in the free lime content after the incorporation of GGBFS and CKD as cement replacement [59].

4.2 Compressive strength

The results of compressive strength of mortar samples of different mixtures subjected to different curing periods are presented in Fig. 4. Generally, there were significant reductions in

the compressive strength after incorporating GGBFS and CKD as cement replacements particularly at the early ages of curing. This reduction can be recognized clearly with the increase of the OPC replacement content. This was due to the slow acquisition of strength at initial curing ages for the mixes containing 40% or higher GGBS [60, 61]. Surprisingly, after the first day of curing, the ternary mixture T40 indicated a compressive strength higher than that of the reference mortar (8.4 and 9.6MPa for the reference cement and T40 respectively). This may be due to high alkalinity provided by sufficient amount of cement for activating the GGBFS quickly. After 7 days of curing, all mixes showed significant developments in the compressive strength; the strength developments achieved were 141%, 170%, 211%, 2.35% and 236% for REF,T20, T40, T60 and T80 respectively (at age of 7 days in referring to age of 3 days). This indicated that as the replacement of cement increased, the progression of the compressive strength increased. This behavior could be attributed to the alkaline activation of the CKD to the grains of GGBFS resulting in compacted structure of the mortars which led to the significant development in the compressive strength [62].

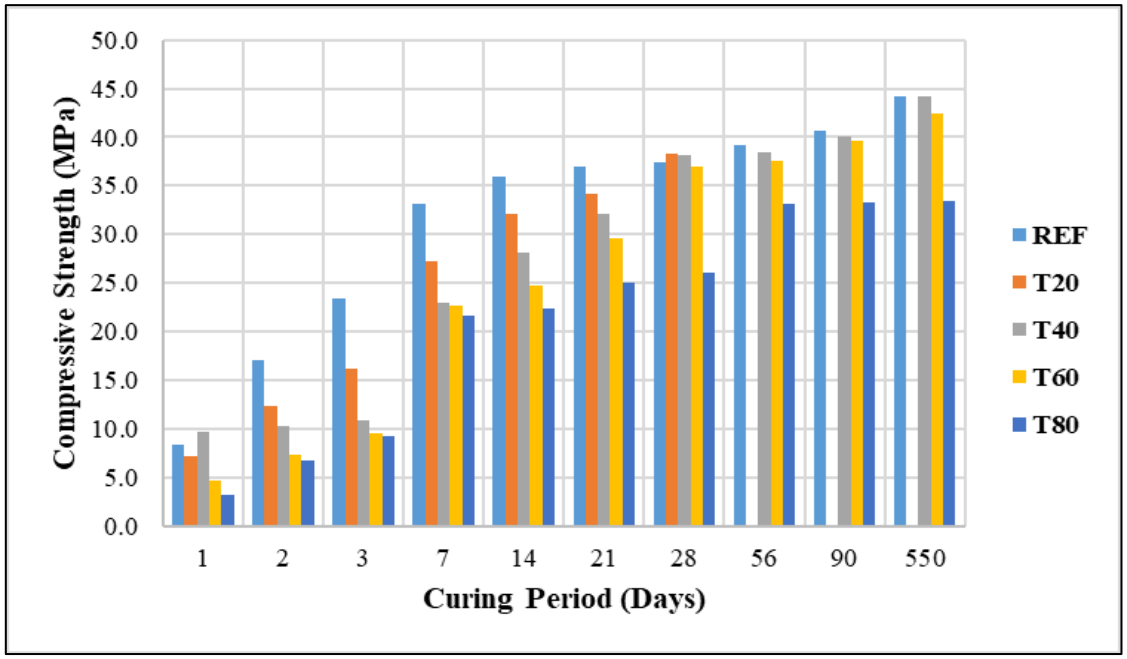

Fig. 4. Development of mortars compressive strength at different ages of curing

For the samples cured for longer than 7 days, the evolution of the compressive strength of the mortars contained GGBFS and CKD became higher than that for the reference cement. This evolution in the compressive strength is attributed to the the formation of additional C-S-H gel from both the chemical reaction occurring between the lime from the CKD and amorphous silica provided by GGBS together with the high alkalinity environment of CKD that enhanced the dissolution of the glassy phases of GGBS producing additional C-S-H gel [26, 63, 64]. This gel tends to fill pores and grow into capillary spaces, resulting in a more impermeable, dense and higher-strength structure [63-65].

Interestingly, the mortars prepared using T40 and T60 indicated compressive strengths closed to that of REF after 28 days of curing onwards. Moreover, ternary mixture T60 indicated a compressive strength comparable to the reference cement after 28 days curing (98.6% of the compressive strength of the mortars prepared from OPC alone). However, a significant reduction in compressive strength was recorded with the use of T80. At the curing age of 550 days, a noticeable increment was observed for the samples prepared from binders T40 and T60 with an acceptable compressive strength of T60 in comparison with that of the reference mortars (T60 indicated a compressive strength equal to 96% of that of OPC). This behavior could be due to the enhancement of the pozzolanic reaction of the GGBFS particles in the presence of the alkaline materials and sulphates produced from CKD at the later ages of curing. Therefore, the use of ternary blending of OPC, GGBFS and CKD can be promising as a construction material in different fields of civil engineering which can perform similar to the conventional binder (OPC).

4.3 Ultrasonic Pulse Velocity (UPV) Test

The results of UPV test performed on cubic mortars of 100X100X100mm prepared from different ternary blended binders in addition to the reference binder (REF) at different curing

ages are presented in Fig. 5. Generally, the results obtained from UPV test were consistent with those obtained from the compressive strength test. For the early ages of curing (1, 2 and 3 days), there were significant reduction in the measured velocity after the incorporation of GGBFS and CKD as cement replacement materials. After 7 days of curing, the results obtained from the UPV test became close to each other for all mixtures including the reference binder. After the first week of curing, the increase in the velocity of the reference sample was marginal indicating the slowdown of the mechanical properties evolution. The velocity measured from the UPV test of the reference sample was 4238 m/s at 14 days age while it became 4304 m/s at 28 days. The development was more pronounced with respect to the samples prepared using the ternary blended mixtures. For example, the velocity measured from the samples prepared using T60 was 4087 m/s at 14 days age and became 4161 m/s at 28 days. Negligible reduction and no change were recorded between 21 and 28 days of curing for mixtures T40 and T80 respectively.

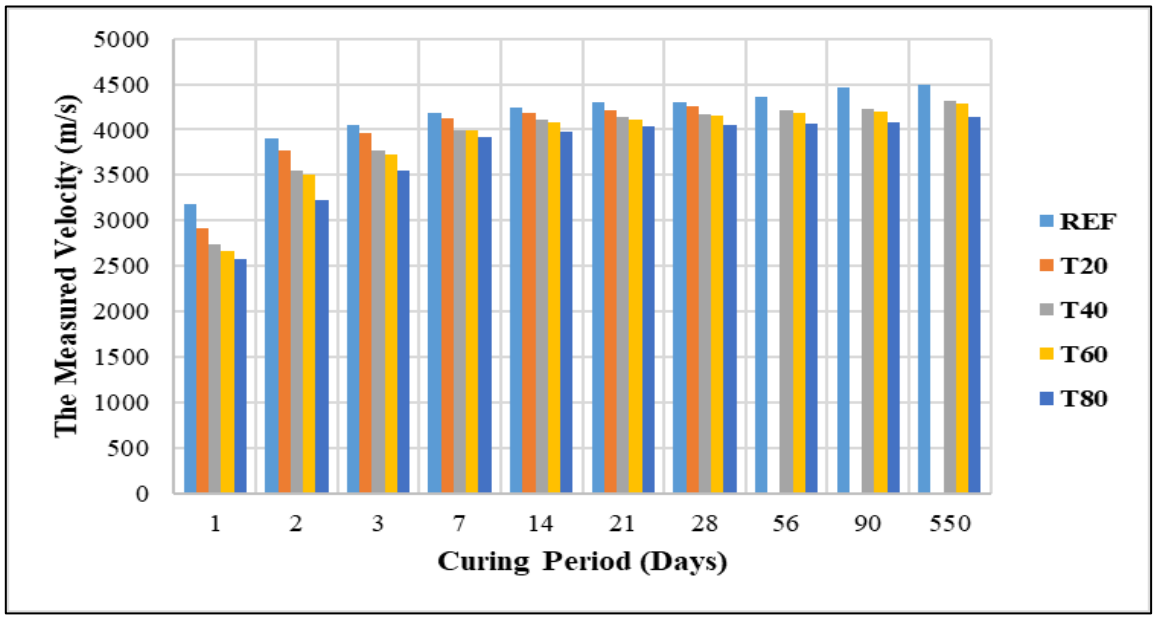

Fig. 5. Development of velocity obtained from UPV test.

From Fig. 5, it can be seen that ternary mixtures T20, T40 and T60 exhibited a performance closed to each other over all curing periods and the performance of both was comparable to the

reference binder. A Similar behavior was reported by Najim et al. [23] after using CKD as a cement replacement to produce concrete samples. They attributed the reduction in UPV values with the increase in CKD content replacing OPC to the increase in the porosity and the decrease in the density of the tested samples. Mohseni et al. [42] reported that mortar has good durability when its UPV value is in the range of 3660–4575 m/s and according to Fig. 5 the mixture T40 and T60 have UPV value higher than 3660 m/s after 3 days of cuing. Therefore, T40 and T60 could be considered as durable mortar [42].

According to the results of the mechanical and durability performance of cement mortars, the mixture T60 was considered as the optimum mixture as it has shown comparable mechanical and durability performance relative to the control mixture (REF) and at the same time it incorporated higher amount of GGBFS and CKD relative to T40.

4.4 Numerical analysis and modelling

4.4.1 Testing the Assumption of MR

Two MR models were developed in this study; the first model employed experimental parameters (curing time and mixture) as EVs to predict the mechanical performance of the mortars (RV) while the second model uses the same parameters predicted the durability performance of the mortars (RV). Researchers [66, 67] confirmed that the rate of mechanical and durability performance development after seven days curing time is lower than that with seven days age or less. Thus, the data set were divided into two sets of seven days age or less and more than seven days for numerical analysis purposes.

To conduct MR analysis, issues surrounding assumptions MR need to be met [30, 33, 49]. The RV should be one scale variable and EVs should be two or more variables measured at a continuous or nominal level [33, 46]. The RVs are scale variables and the mixture is a nominal variable with four categories (REF, T40, T60 and T80). These variables meet the assumption

of MR. However, the curing time variable is ordinal with 10 categories, which violates this assumption. Tabachnick and Fidell [33] and [49] stated that the ordinal variable can be treated as a scale variable or as a nominal variable during MR; thus, the curing time was treated as a nominal with 10 categories during analysis. Besides, Tabachnick and Fidell, [33] recommend the use of dummy variable coding to find linear relationships between nominal variables and continues (scale) variables. Dummy coding is the conversion of a discrete variable with more than two categories into a series of dichotomous ones (one fewer than its categories) that takes the value 0 or 1 to indicate the absence or presence of the categorical effect [46, 49]. Thus, three dichotomous variables were created to represent the four categories of mixtures and nine dichotomous variables were created to represent the ten categories of curing time. Thus, the design assumption of MR has been met.

The sample size should be substantial to produce a generalizable prediction model [33, 46]. According to Eq. (2), the smallest sample size to develop a generalizable prediction model using MR technique is 66 observations, tacking in to account that two variables (curing time and mixture) were used as EVs [30, 33]. This requirement was met as 160 observations were collected for mortars' mechanical performance analysis and similar dataset size was used for the durability performance analysis.

Additionally, the existence of collinearity among all dummy variables that represent both EVs was examined by calculating the tolerance value for each dummy variable. The results of collinearity test showed that all dummy variables met the collinearity assumptions as the values of tolerance were greater than 0.1 (Table 5).

However, the outcome of the Kolmogorov-Smirnov test for both RVs (mechanical and durability performance) showed that these variables do not follow a normal distribution (the p-value was 0.000 for both RVs) which is less than the threshold value of 0.05 [46, 47]. The

448 inverse square root function [33, 49] has been used to mathematically normalised both RVs to
449 increase the p-values to a minimum of 0.069 which in turn confirms the normality.
450
451
452
453
454
455
456
457
458
459
460
461
462
463
464
465
466

467 Table 5: summary of statistical analysis

Model	Parameters' dummies	Tolerance	*P*-value	Presence of outliers		Maximum Mahalanobis Distance
				Cases' number	Standardised residuals	
Compressive strength	REF [a]	-	-	27	4.223	7.917
	T40	0.667	0.000			
	T60	0.667	0.000			
	T80	0.667	0.000			
	CT1 [a]	-	-			
	CT2	0.556	0.000			
	CT3	0.556	0.000			
	CT7	0.556	0.000			
	CT14 [a]	-	-			
	CT21	0.556	0.001			
	CT28	0.556	0.000			
	CT56	0.556	0.000			
	CT90	0.556	0.000			
	CT550	0.556	0.000			
Durability	REF [a]	-	-	14 35 36	7.773 3.348 3.308	5.906
	T40	0.667	0.000			
	T60	0.667	0.000			
	T80	0.667	0.000			
	CT1 [a]	-	-			
	CT2	0.556	0.000			
	CT3	0.556	0.000			
	CT7	0.556	0.000			
	CT14 [a]	-	-			
	CT21	0.556	0.000			
	CT28	0.556	0.000			
	CT56	0.556	0.000			
	CT90	0.556	0.000			
	CT550	0.556	0.000			

468 a. This is a reference category for comparison purposes.

Additionally, Table 5 shows that there is one outlier within the mechanical performance model (residual exceeded the range of ±3.3) and three cases within the durability performance model. Tabachnick and Fidell [33] recommend the uses of Mahalanobis Distance and Cooks' Distance to understand the influence of these cases on the outcome of developed models. Pallant [46] stated that the outlying cases must be excluded if the Mahalanobis Distance and Cooks' Distance exceed the threshold values of 13.82 and 1, respectively; otherwise, the cases have an insignificant influence on the developed models. Thus, both distances were calculated to check whether or not the outlying cases in both models exert significant influences. Table 5 showed that the Mahalanobis Distance values for both models were below the threshold value, indicating that the outliers do not exert a significant influence. Besides, the Cooks' Distances were 0.226 and 0.448 for mechanical and durability performance models, respectively, confirming that the cases have a negligible influence on the predictability of the proposed MR models. Therefore, these cases were kept in the models due to their minor influence.

4.4.2 Contribution of EVs and Models' performance

Based on the results of the statistical analyses, two MR models were developed to predict mortars' mechanical and durability performance. Equations (4) and (5) show the influence of the studied parameters (curing time and mixture) on the development of the mechanical and durability performance of the mortars.

$$\begin{aligned} Mechanical \; = \Omega(1.751 \; - \; 0.284\,T40 - \; 0.320\,T60 - \; 0.371\,T80 \; + \; 0.239\,CT2 \quad (4) \\ + \; 0.363\,CT3 + \; 0.724\,CT7)^4 \\ + \; \mathcal{L}(45.33 \; - \; (3.571 \; + \; 0.458\,T40 + \; 0.655\,T60 + \; 1.423\,T80 \\ - \; 0.443\,CT21 \; - \; 1.238\,CT28 - \; 1.351\,CT56 \; - \; 1.631\,CT90 \\ - \; 2.389\,CT550)^2) \end{aligned}$$

$$Durablity = \Omega(4250 - (30.896 + 8.215\,T40 + 8.835\,T60 + 11.695\,T80 - 11.971\,CT2 - 16.804\,CT3 - 24.098\,CT7)^2) + \mathcal{L}(4261.77 - 161.35\,T40 - 187.958\,T60 - 300.714\,T80 + 43.125\,CT21 + 72.459\,CT28 + 110.014\,CT56 + 141.104\,CT90 + 201.312\,CT550) \quad (5)$$

Where Ω and $\mathcal{L}$ are the combination factors, with values given in Equations (6) and (7):

$$\Omega = \begin{cases} 1 \ when\ CT \ \leq 7\ days \\ 0\ when\ CT > 7\ days \end{cases} \quad (6)$$

$$\mathcal{L} = \begin{cases} 0 \ when\ CT \ \leq 7\ days \\ 1\ when\ CT > 7\ days \end{cases} \quad (7)$$

The contribution of each EV to the outcome of the developed models was evaluated through the use of the regression coefficient (*m*) and the statistical significance (*p*-value) [33, 46, 49]. Table 5 shows that all the employed EVs have *p*-values of 0.001 or less suggesting that the effect of each EV to the RV is statistically significant. Besides, the regression coefficient provides proper information about the effect of each individual EV to the RV [30, 33, 47]. It can be clearly seen from equation 4 that the mechanical performance of the mortars increases with the increase in the curing time (the coefficients of the curing time increase with the increase in curing time). For example, the square root of the compressive strength is higher by 2.398 at age of 550 days compared to the age of 14 days; similarly, the fourth root of the compressive strength is higher by 0.724 at age of 7 days compared to the age of one day. Equation 5 also shows that curing time significantly influences the durability performance of the mortars e.g. the durability is higher by 200 unit (m/s) at age of 550 days compared to 14 days of curing time.

Mixtures' materials influence varies according to the fractions of waste materials used. Generally, it can be said that the use of waste materials lowers the mechanical and durability performance of the mortars. However, the numerical analysis showed that both T40 and T60 mixtures achieve comparable mechanical and durability performance (the regression coefficients are comparable for both mixtures) to that achieved by the control mixture despite the fact that 40% and 60% of the OPC was replaced by waste materials, respectively. On the other hand, mixture T80 show a significant drop in both mechanical and durability performance compared to the control mixture, particularly after 7 days of curing time. The regression coefficients of mixture T80 dramatically larger than that observed for other mixtures, suggesting that the mechanical and durability performance of the mortars are dramatically dropped. The numerical analysis results support the claim that T60 was the optimum mixture as it has shown comparable mechanical and durability performance relative to the control mixture and at the same time it incorporated 60% of waste materials.

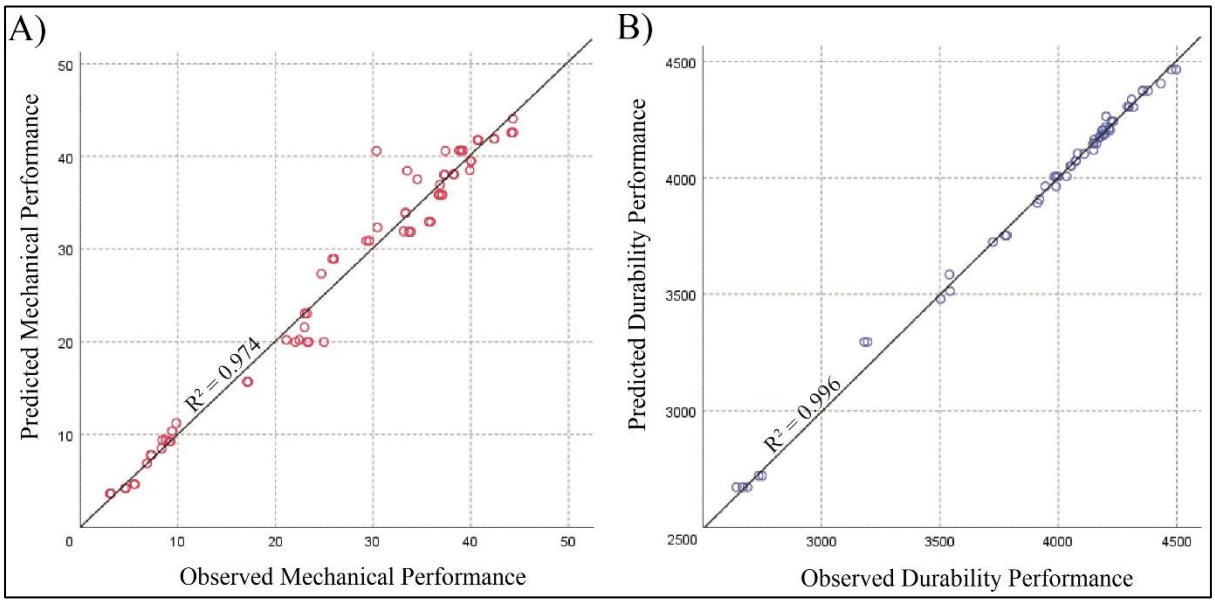

Fig. 6: Relationships between predicted and observed mortars' properties: A) the mechanical performance of the mortars and B) the durability performance of the mortars.

To evaluate the performance of the proposed production models, about 40% of each dataset was randomly selected using random sampling function in SPSS-26 software to avoid statistical bias. 67 cases were used to evaluate the performance of the compressive strength prediction model while 57 cases were used to evaluate the performance of the durability prediction model. Fig. 6 reveals both models achieved a high level of agreement between the predicted and observed RV, the R^2 values for both models were higher than 0.97. This confirms that both models were able to explain more than 97% of the variance in the mechanical and durability performance of the mortars.

4.5 Scanning Electron Microscopy (SEM) and Energy Dispersive X-ray Spectroscopy (EDX) Testing

The micrographs of the hydrated pastes of the selected binder (T60) after they were subjected to different curing periods are presented in Fig. 7. At the early ages of hydration (1, 3 and 7 days) the formation of needle shape particles (Ettringite) as well as the platy shape of Portlandite (CH) can be observed easily which gives an indication of the reactivity of the used binder to enhance the mechanical properties of the produced mortars [45, 57]. However, the SEM image of the 3 and 7 days aged paste indicated the formation of the cementitious gel (Calcium Silicate Hydrate (C-S-H)) that is the main strength-generating material responsible for providing the binding and strengthening properties of the mix and it contributes the early compressive gained along with the Ettringite [26]. Moreover, the pore voids at the early ages of curing can be recognized in the morphology of the examined pastes. These findings are agreed with those reported by Chaunsali and Peethamparan [68]. With the progression of the hydration time, the microstructure of the T60 paste becomes denser and more coherent. As it can be seen from Fig. 7, at 28 days of hydration, the hydration gel (C-S-H) is the dominant and there is no presence for both the Etrringite and CH particles. A very dense and coherent

541 microstructure was gained after longer curing period (90 and 550 days) which indicated that
542 cementitious gel (C-S-H) almost covered the sample without any noticeable pore voids. This
543 can give an understanding about the development of the compressive strength of the produced
544 mortars using the binder T60 as well as the well durable performance after extended curing
545 period.

546

547

548

549

550

551

552

553

554

555

556

557

558

559

560

561

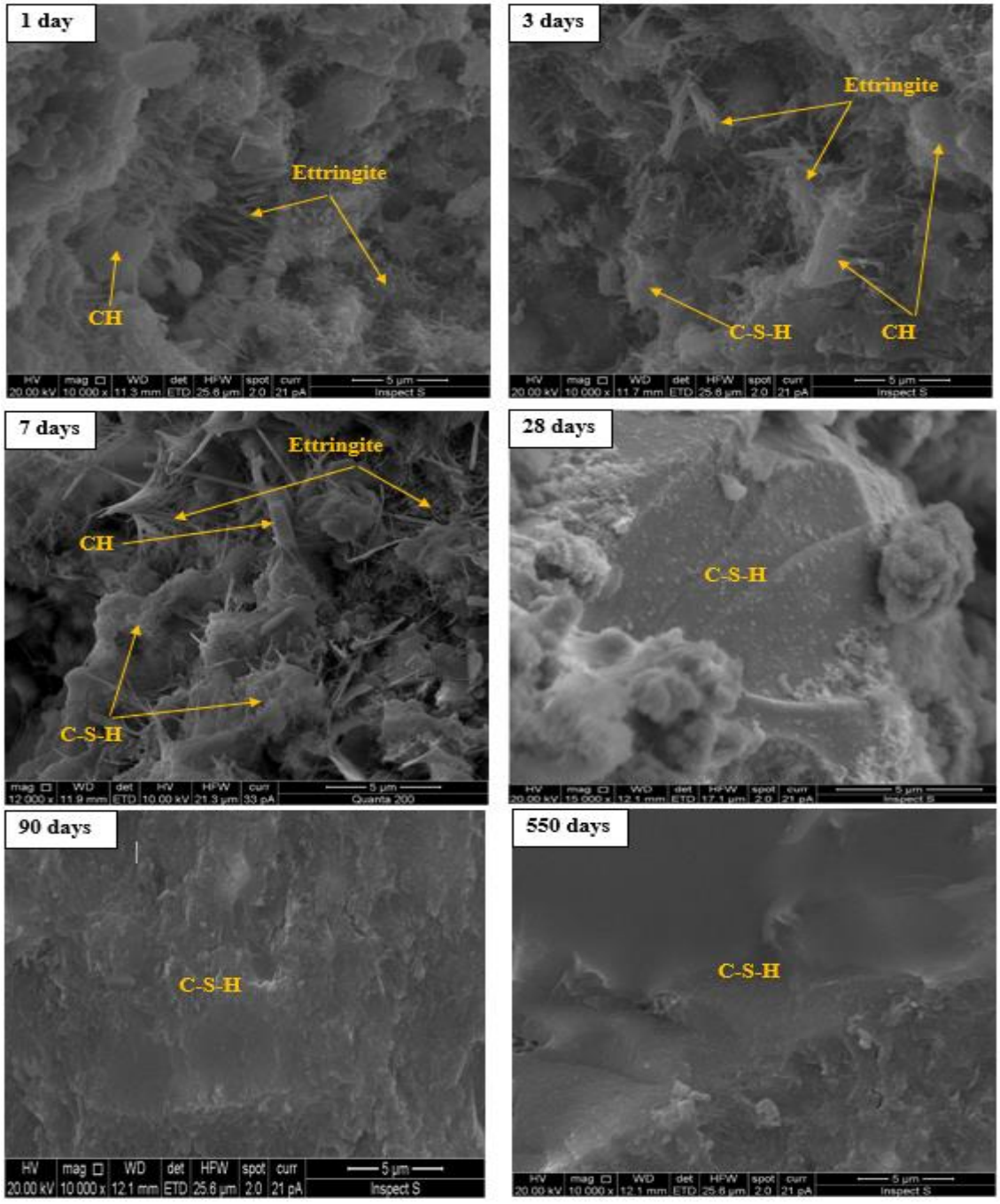

562

563 Fig. 7. SEM images of the paste of binder T60 at different ages of curing.

564

565

566

Figs. 8-11 presented the EDX spectrum of C-S-H paste of the T60 mixture from 1 to 28 days of curing. At all curing ages, the principle peaks were Ca and Si with trace amounts of Al, K, Mg, Cl and S. The obtained EDX spectrum of the C-S-H phase were similar with the EDX spectrum reported previously by Peethamparan et al. [69] and Harbec et al. [70]. Sadique and Al-Nageim [71] reported that the concentration of the calcium in the C-S-H gel reflects the density and stability of the cementitious product. It can be seen from Table 6 that the Ca content was high at all curing ages and Na was only detected at the age of 3 days, thus the formed C-S-H gel is very stable according to Sadique and Al-Nageim [71] who have reported that more stable gel with less deleterious expansion forms at higher Ca content and lower K and Na contents. Additionally, the availability of high Ca and Si contents of the T60 paste at different ages of curing gives an indication about the continues formation of C-S-H gel that significantly increases the strength and durability of the binder. This is in agreement with the improvement in the strength and durability performance of the T60 mortar with increasing the period of curing.

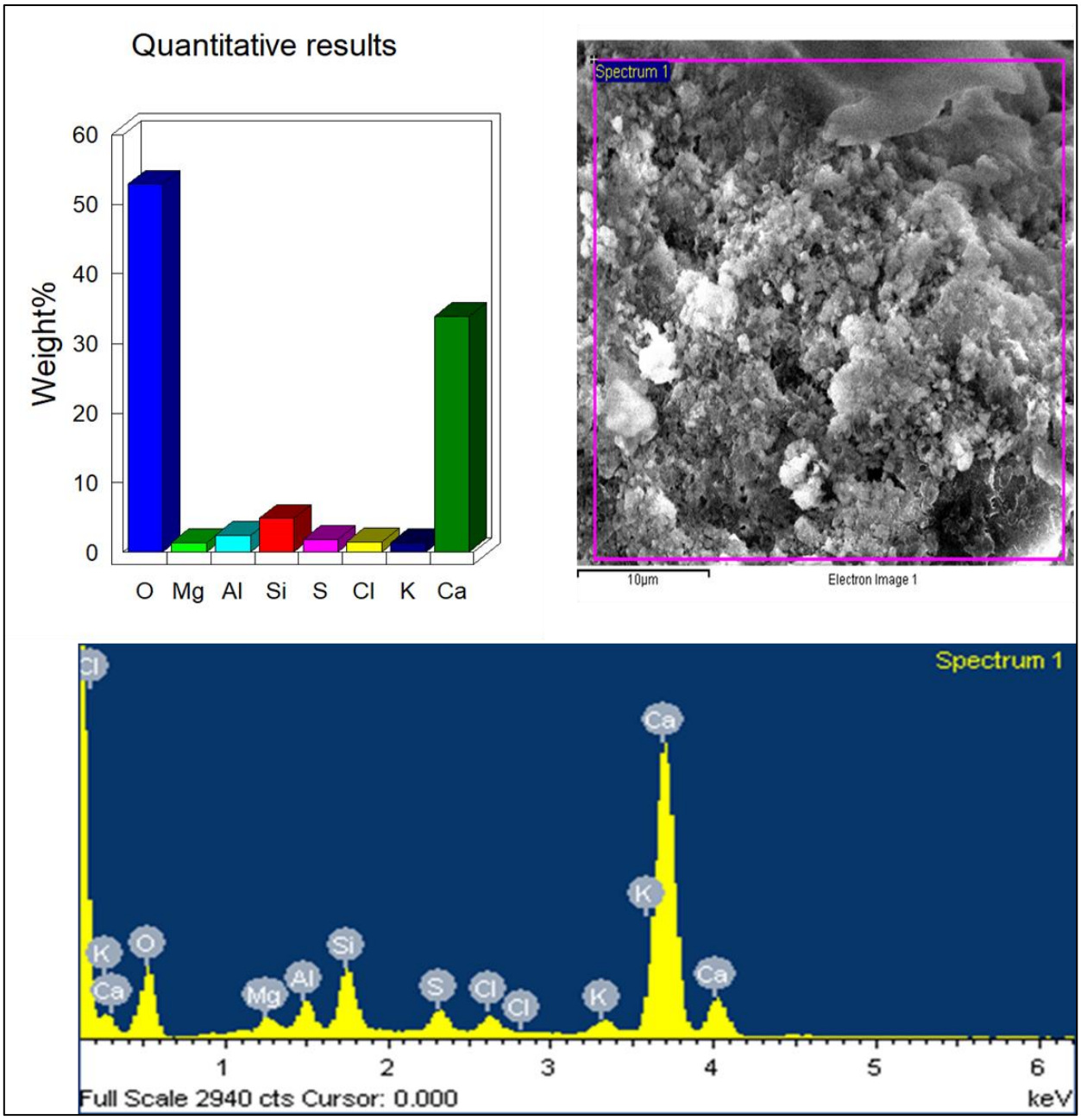

Fig. 8. EDX spectrum of T60 paste at 1 day curing

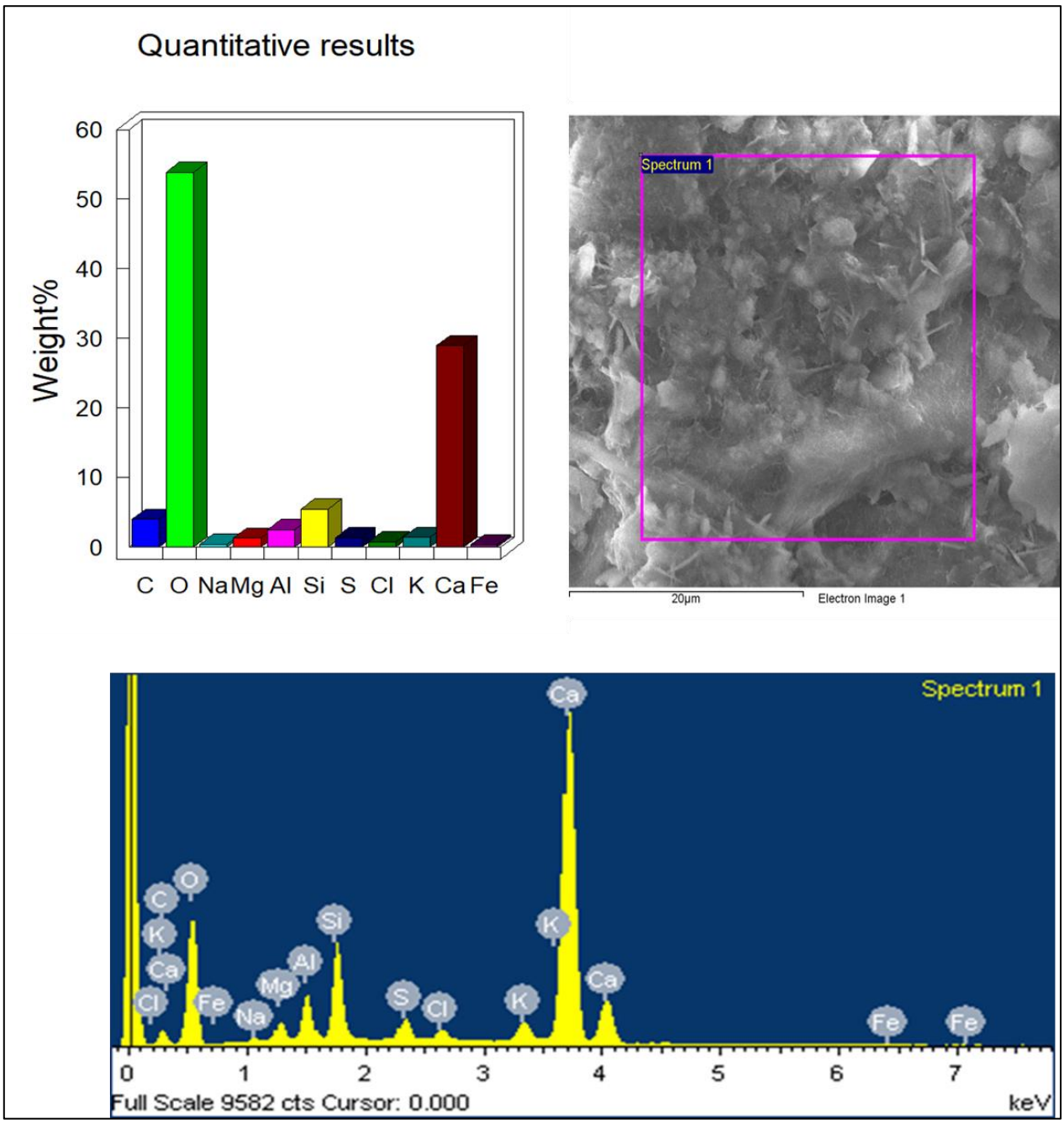

Fig. 9. EDX spectrum of T60 paste at 3 days curing

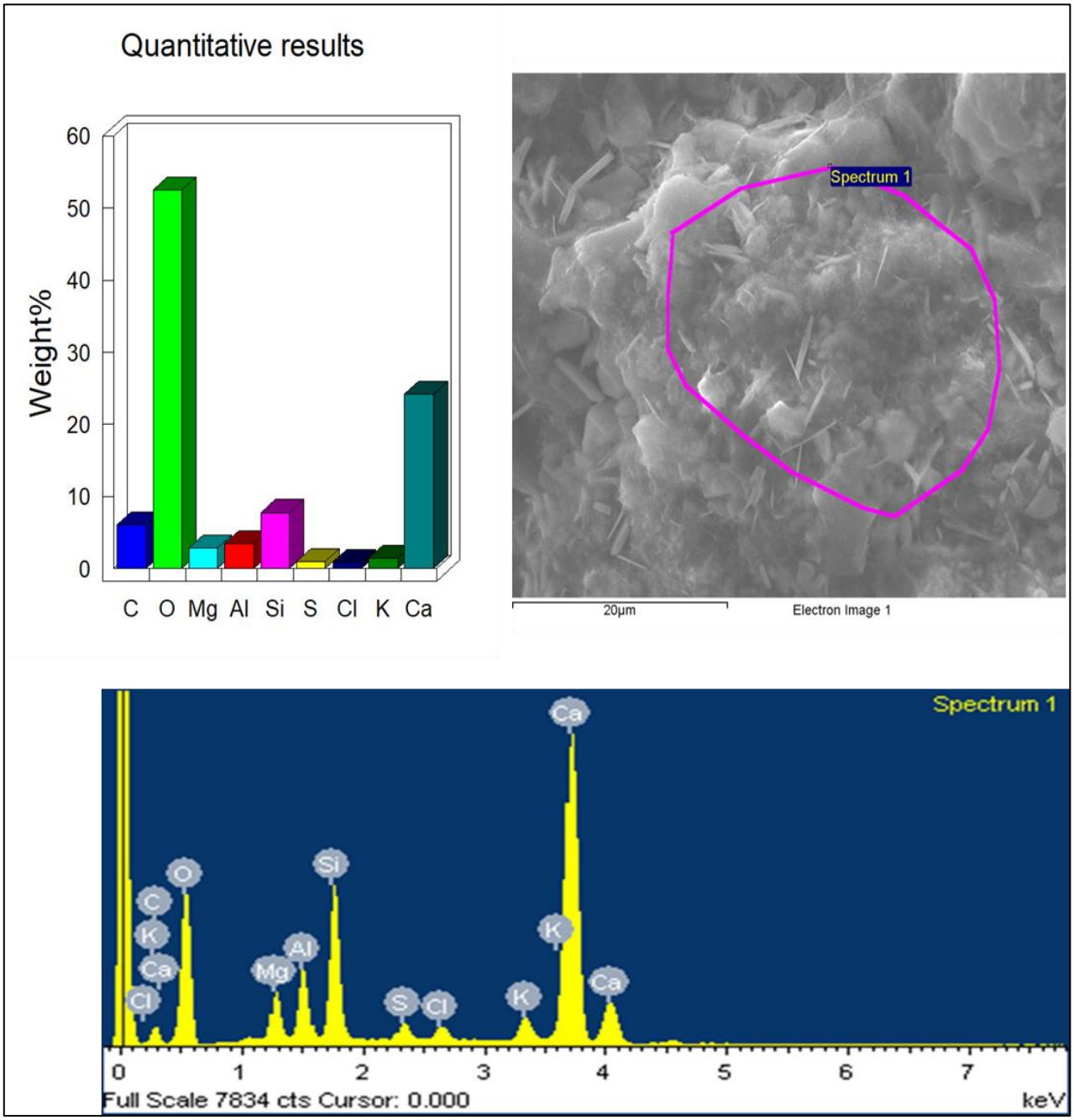

Fig. 10. EDX spectrum of C-S-H paste at 7 days curing

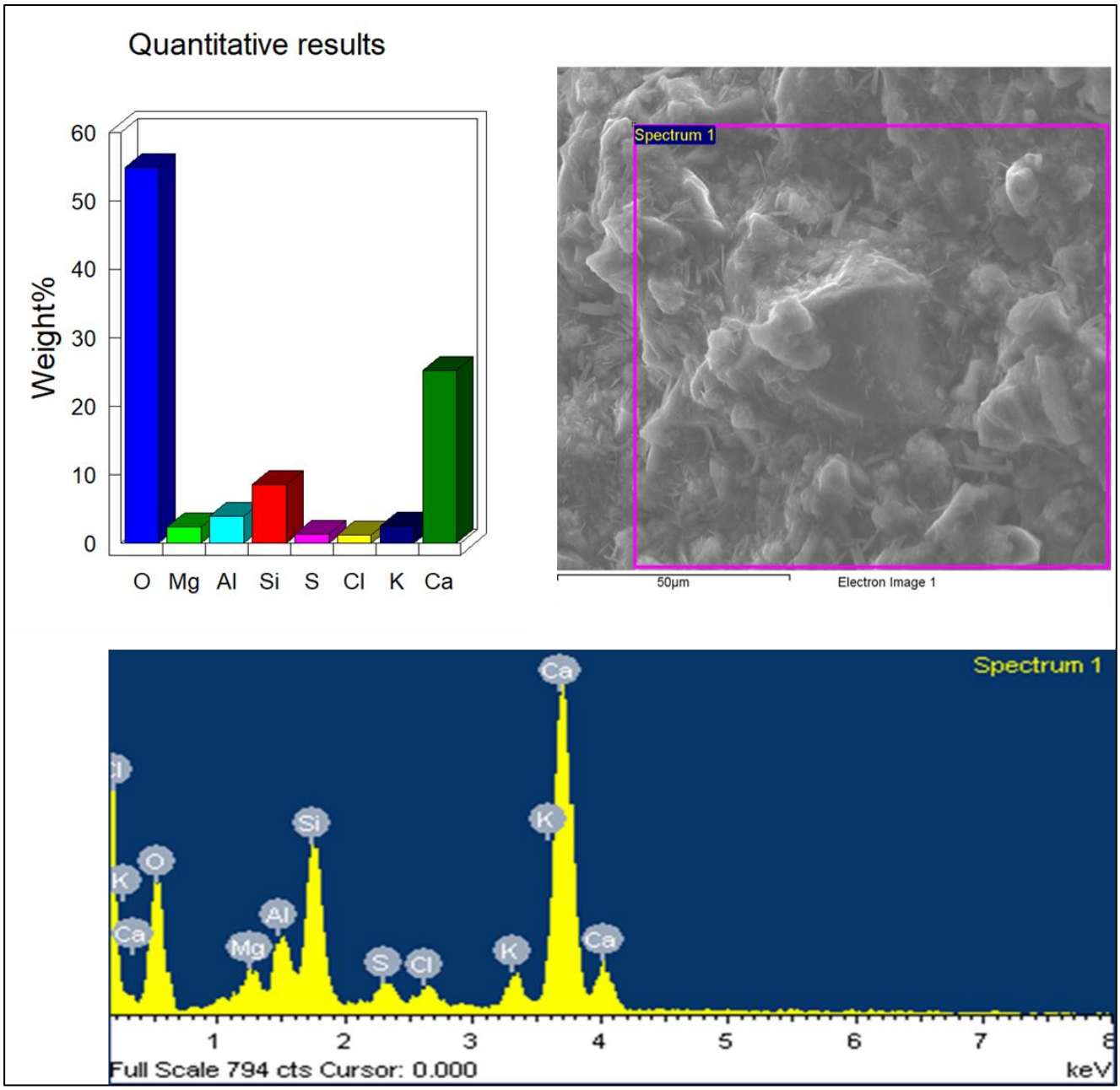

Fig. 11. EDX spectrum of T60 paste at 28 days curing

670 Table 6. EDX analysis of T60 paste after different periods of hydration reaction

	1 day		**3 days**		**7 days**		**28 days**	
Element	Weight %	Atomic %	Weight %	Atomic %	Weight %	Atomic %	Weight %	Atomic %
C	-	-	3.97	6.79	6.04	10.07	-	-
O	52.89	71.85	53.85	69.07	52.52	65.65	54.95	72.32
Na	-	-	0.35	0.31	-	-	-	-
Mg	1.36	1.22	1.26	1.06	2.83	2.33	2.36	2.05
Al	2.43	1.95	2.5	1.9	3.47	2.57	3.93	3.07
Si	4.83	3.73	5.42	3.96	7.77	5.54	8.57	6.42
S	1.87	1.27	1.31	0.84	0.94	0.59	1.29	0.85
Cl	1.48	0.9	0.71	0.41	0.86	0.49	1.19	0.71
K	1.32	0.74	1.39	0.73	1.43	0.73	2.47	1.33
Ca	33.82	18.34	28.95	14.82	24.12	12.03	25.23	13.26
Fe	-	-	0.28	0.1	-	-	-	-

671

672

673

674

5. Conclusion

This research project was devoted to study the effect of cement substitution with two different by-product materials (GGBFS and CKD) on some of the mechanical, durability and microstructural properties of cement mortar. Based on the results obtained from different experimental and statistical works performed in this research study, the following conclusions can be drawn:

- Increasing the GGBFS and CKD content resulted in increasing the water demand and extending the initial and final setting times relative to the control mixture.
- At early ages (1, 2, 3, 7 days), increasing the GGBFS and CKD content caused a significant reduction in the compressive strength and durability of cement mortar. However, at the age of 28 days onwards, replacing the cement with up to 60% GGBFS and CKD resulted in comparable compressive strength and durability performance relative to the control mixture.
- Replacing the cement with 80% GGBFS and CKD caused a considerable reduction in the mechanical and durability performance of the mortars relative to the control mortar.
- The optimum synthesis of binder materials in this research was chosen to be (40% OPC: 40%GGBFS: 20% CKD).
- The SEM and EDX analysis of the optimum synthesis of binder materials (T60) confirmed the results of the compressive strength and durability tests.
- The results of the numerical analysis were well in agreement with the results from the experimental work with a coefficient of determination (R^2) of more than 0.97.
- Regarding all tests considered in this study, it can be concluded that replacing the cement by 60% GGBFS and CKD will contribute to produce a sustainable mortar with comparable durability and mechanical performance and at the same time it can

significantly contributes to decrease the cost of construction materials and reduce the CO_2 emissions into the atmosphere.

Conflict of interest

None.

Acknowledgments

The laboratory support for this research provided by Liverpool John Moors University, UK is gratefully acknowledged.

References

[1] Gaffey, M.F., J.K. Das, and Z.A. Bhutta, *Millennium Development Goals 4 and 5: Past and future progress.* Semin Fetal Neonatal Med, 2015. **20**(5): p. 285-92.

[2] Mehta, A. and D.K. Ashish, *Silica fume and waste glass in cement concrete production: A review.* Journal of Building Engineering, 2019: p. 100888.

[3] Specht, E., T. Redemann, and N. Lorenz, *Simplified mathematical model for calculating global warming through anthropogenic CO 2.* International Journal of Thermal Sciences, 2016. **102**: p. 1-8.

[4] Karim, M.R., M.F.M. Zain, M. Jamil, and F.C. Lai, *Fabrication of a non-cement binder using slag, palm oil fuel ash and rice husk ash with sodium hydroxide.* Construction and Building Materials, 2013. **49**: p. 894-902.

[5] Saedi, M., K. Behfarnia, and H. Soltanian, *The effect of the blaine fineness on the mechanical properties of the alkali-activated slag cement.* Journal of Building Engineering, 2019. **26**: p. 100897.

[6] van Ruijven, B.J., D.P. van Vuuren, W. Boskaljon, M.L. Neelis, D. Saygin, and M.K. Patel, *Long-term model-based projections of energy use and CO2 emissions from the global steel and cement industries.* Resources, Conservation and Recycling, 2016. **112**: p. 15-36.

[7] Shubbar, A.A., M. Sadique, H.K. Shanbara, and K. Hashim, *The Development of a New Low Carbon Binder for Construction as an Alternative to Cement*, in *Advances in Sustainable Construction Materials and Geotechnical Engineering*. 2020, Springer. p. 205-213.

[8] Younes, M., H. Abdel-Rahman, and M.M. Khattab, *Utilization of rice husk ash and waste glass in the production of ternary blended cement mortar composites.* Journal of Building Engineering, 2018. **20**: p. 42-50.

[9] Aprianti, E., P. Shafigh, S. Bahri, and J.N. Farahani, *Supplementary cementitious materials origin from agricultural wastes – A review.* Construction and Building Materials, 2015. **74**: p. 176-187.

[10] Aprianti S, E., *A huge number of artificial waste material can be supplementary cementitious material (SCM) for concrete production – a review part II.* Journal of Cleaner Production, 2017. **142**: p. 4178-4194.

[11] Kotwica, Ł., W. Pichór, E. Kapeluszna, and A. Różycka, *Utilization of waste expanded perlite as new effective supplementary cementitious material.* Journal of Cleaner Production, 2017. **140**: p. 1344-1352.
[12] Horpibulsuk, S., C. Phetchuay, A. Chinkulkijniwat, and A. Cholaphatsorn, *Strength development in silty clay stabilized with calcium carbide residue and fly ash.* Soils and Foundations, 2013. **53**(4): p. 477-486.
[13] McNally, C. and E. Sheils, *Probability-based assessment of the durability characteristics of concretes manufactured using CEM II and GGBS binders.* Construction and Building Materials, 2012. **30**: p. 22-29.
[14] Ghosh, A. and C. Subbarao, *Strength Characteristics of Class F Fly Ash Modified with Lime and Gypsum.* Journal Of Geotechnical And Geoenvironmental Engineering, 2007. **133**(7): p. 757-766.
[15] Shubbar, A.A., M. Sadique, P. Kot, and W. Atherton, *Future of clay-based construction materials – A review.* Construction and Building Materials, 2019. **210**: p. 172-187.
[16] Shubbar, A., H.M. Jafer, A. Dulaimi, W. Atherton, and A. Al-Rifaie, *The Development of a Low Carbon Cementitious Material Produced from Cement, Ground Granulated Blast Furnace Slag and High Calcium Fly Ash.* International Journal of Civil, Environmental, Structural, Construction and Architectural Engineering, 2017. **11**(7): p. 905-908.
[17] Karthik, A., K. Sudalaimani, and C.T. Vijaya Kumar, *Investigation on mechanical properties of fly ash-ground granulated blast furnace slag based self curing bio-geopolymer concrete.* Construction and Building Materials, 2017. **149**: p. 338-349.
[18] Sargent, P., P.N. Hughes, M. Rouainia, and M.L. White, *The use of alkali activated waste binders in enhancing the mechanical properties and durability of soft alluvial soils.* Engineering Geology, 2013. **152**(1): p. 96-108.
[19] Hawileh, R.A., J.A. Abdalla, F. Fardmanesh, P. Shahsana, and A. Khalili, *Performance of reinforced concrete beams cast with different percentages of GGBS replacement to cement.* Archives of Civil and Mechanical Engineering, 2017. **17**(3): p. 511-519.
[20] Divsholi, B.S., T.Y.D. Lim, and S. Teng, *Durability Properties and Microstructure of Ground Granulated Blast Furnace Slag Cement Concrete.* International Journal of Concrete Structures and Materials, 2014. **8**(2): p. 157-164.
[21] Duan, P., Z. Shui, W. Chen, and C. Shen, *Enhancing microstructure and durability of concrete from ground granulated blast furnace slag and metakaolin as cement replacement materials.* Journal of Materials Research and Technology, 2013. **2**(1): p. 52-59.
[22] Najim, K.B., Z.S. Mahmod, and A.-K.M. Atea, *Experimental investigation on using Cement Kiln Dust (CKD) as a cement replacement material in producing modified cement mortar.* Construction and Building Materials, 2014. **55**: p. 5-12.
[23] Najim, K.B., I. Al-Jumaily, and A.M. Atea, *Characterization of sustainable high performance/self-compacting concrete produced using CKD as a cement replacement material.* Construction and Building Materials, 2016. **103**: p. 123-129.
[24] Mosa, A.M., A.H. Taher, and L.A. Al-Jaberi, *Improvement of poor subgrade soils using cement kiln dust.* Case Studies in Construction Materials, 2017. **7**: p. 138-143.
[25] Amin, M.S. and F.S. Hashem, *Hydration characteristics of hydrothermal treated cement kiln dust–sludge–silica fume pastes.* Construction and Building Materials, 2011. **25**(4): p. 1870-1876.
[26] Sadique, M., H. Al Nageim, W. Atherton, L. Seton, and N. Dempster, *A new composite cementitious material for construction.* Construction and Building Materials, 2012. **35**: p. 846-855.
[27] Khalil, E.A.B. and M. Anwar, *Carbonation of ternary cementitious concrete systems containing fly ash and silica fume.* Water Science, 2015. **29**(1): p. 36-44.

[28] Hashim, K.S., A. Shaw, R. Al Khaddar, M. Ortoneda Pedrola, and D. Phipps, *Defluoridation of drinking water using a new flow column-electrocoagulation reactor (FCER) - Experimental, statistical, and economic approach.* J Environ Manage, 2017. **197**: p. 80-88.
[29] Hashim, K.S., A. Shaw, R. Al Khaddar, M.O. Pedrola, and D. Phipps, *Iron removal, energy consumption and operating cost of electrocoagulation of drinking water using a new flow column reactor.* J Environ Manage, 2017. **189**: p. 98-108.
[30] Abdulredha, M., R. Al Khaddar, D. Jordan, P. Kot, A. Abdulridha, and K. Hashim, *Estimating solid waste generation by hospitality industry during major festivals: A quantification model based on multiple regression.* Waste Management, 2018. **77**: p. 388-400.
[31] Jafer, H.M., K.S. Hashim, W. Atherton, and A.W. Alattabi, *A Statistical Model for the Geotechnical Parameters of Cement-Stabilised Hightown's Soft Soil: A Case Study of Liverpool, UK.* International Journal of Civil, Environmental, Structural, Construction and Architectural Engineering, 2016. **10**(7): p. 885 - 890.
[32] Alattabi, A.W., C.B. Harris, R.M. Alkhaddar, K.S. Hashim, M. Ortoneda-Pedrola, and D. Phipps, *Improving sludge settleability by introducing an innovative, two-stage settling sequencing batch reactor.* Journal of Water Process Engineering, 2017. **20**: p. 207-216.
[33] Tabachnick, B.G. and L.S. Fidell, *Using multivariate statistics*. 2013, Boston: Pearson Education.
[34] BSI, *BS EN 197-1: 2011.* Cement, Composition, Specifications and Conformity Criteria for Common Cements. London, England: British Standard Institution (BSI), 2011.
[35] Celik, O., E. Damci, and S. Paskin, *Characterisation of fly ash and its effect on the compressive strength properties of portland cement.* Indian Journal of Engineering & Materials Science 2008. **15**(5): p. 433-440.
[36] Jafer, H.M., W. Atherton, M. Sadique, F. Ruddock, and E. Loffill, *Development of a new ternary blended cementitious binder produced from waste materials for use in soft soil stabilisation.* Journal of Cleaner Production, 2018. **172**: p. 516-528.
[37] Shubbar, A.A., H. Jafer, A. Dulaimi, K. Hashim, W. Atherton, and M. Sadique, *The development of a low carbon binder produced from the ternary blending of cement, ground granulated blast furnace slag and high calcium fly ash: An experimental and statistical approach.* Construction and Building Materials, 2018. **187**: p. 1051-1060.
[38] Dhir, R., T. Dyer, and J. Halliday, *Activation and acceleration of Portland cement/GGBS blends using cement kiln dust (CKD)*, in *Modern Concrete Materials: Binders, Additions and Admixtures*. 1999, Thomas Telford Publishing. p. 361-370.
[39] Hester, D., C. McNally, and M. Richardson, *A study of the influence of slag alkali level on the alkali–silica reactivity of slag concrete.* Construction and Building Materials, 2005. **19**(9): p. 661-665.
[40] British Standard Institution, *Method of testing cement. Determination of setting time and soundness, BS EN 196-3 and A1*. 2008, British Standard Institution.: London
[41] BSI, *Methods of testing cement–Part 1: Determination of strength*. 2005, British Standard Inistitute: London.
[42] Mohseni, E., F. Naseri, R. Amjadi, M.M. Khotbehsara, and M.M. Ranjbar, *Microstructure and durability properties of cement mortars containing nano-TiO2 and rice husk ash.* Construction and Building Materials, 2016. **114**: p. 656-664.
[43] BSI, *BS 1881-203: Part 203: Recommendations for measurement of velocity of ultrasonic pulses in concrete*. 1986, BSI: LONDON.
[44] Salih, M.A., N. Farzadnia, A.A. Abang Ali, and R. Demirboga, *Development of high strength alkali activated binder using palm oil fuel ash and GGBS at ambient temperature.* Construction and Building Materials, 2015. **93**: p. 289-300.
[45] Dodds, L., *Microstructure Characterisation of Ordinary Portland Cement Composites for the Immobilisation of Nuclear Waste*, in *Faculty of Engineering and Physical Sciences*. 2012, University of Manchester: UK.

[46] Pallant, J., *SPSS Survival Manual 4th edition: A step by step guide to data analysis using SPSS version 18: Maidenhead, Berkshire.* Open University Press. Retrieved on, 2011. **10**(05): p. 2012.
[47] Hashim, K.S., R. Al Khaddar, N. Jasim, A. Shaw, D. Phipps, P. Kot, M.O. Pedrola, A.W. Alattabi, M. Abdulredha, and R. Alawsh, *Electrocoagulation as a green technology for phosphate removal from river water.* Separation and Purification Technology, 2019. **210**: p. 135-144.
[48] Thanh, N.P., Y. Matsui, and T. Fujiwara, *Household solid waste generation and characteristic in a Mekong Delta city, Vietnam.* J Environ Manage, 2010. **91**(11): p. 2307-21.
[49] Laerd Statistics. *Binomial logistic regression using spss statistics* 2015; Available from: https://statistics.laerd.com/premium/spss/blr/binomial-logistic-regression-in-spss-15.php
[50] Shubbar, A.A., A. Al-Shaer, R.S. AlKizwini, K. Hashim, H. Al Hawesah, and M. Sadique, *Investigating the influence of cement replacement by high volume of GGBS and PFA on the mechanical performance of cement mortar*, in *International Conference on Civil and Environmental Engineering Technologies, Kufa University, Iraq, 23-24 April*. 2019.
[51] Dave, N., Misra, A. K., Srivastava, A. & Kaushik, S. K.,, *Experimental analysis of strength and durability properties of quaternary cement binder and mortar.* Construction and Building Materials, 2016. **107**: p. 117-124.
[52] Barnett, S.J., M.N. Soutsos, S.G. Millard, and J.H. Bungey, *Strength development of mortars containing ground granulated blast-furnace slag: Effect of curing temperature and determination of apparent activation energies.* Cement and Concrete Research, 2006. **36**(3): p. 434-440.
[53] Chindaprasirt, P. and S. Rukzon, *Strength, porosity and corrosion resistance of ternary blend Portland cement, rice husk ash and fly ash mortar.* Construction and Building Materials, 2008. **22**(8): p. 1601-1606.
[54] Intharathirat, R., P. Abdul Salam, S. Kumar, and A. Untong, *Forecasting of municipal solid waste quantity in a developing country using multivariate grey models.* Waste Manag, 2015. **39**: p. 3-14.
[55] Azadi, S. and A. Karimi-Jashni, *Verifying the performance of artificial neural network and multiple linear regression in predicting the mean seasonal municipal solid waste generation rate: A case study of Fars province, Iran.* Waste Manag, 2016. **48**: p. 14-23.
[56] Siddique, R. and A. Rajor, *Strength and microstructure analysis of bacterial treated cement kiln dust mortar.* Construction and Building Materials, 2014. **63**: p. 49-55.
[57] Sadique, M., H. Al-Nageim, W. Atherton, L. Seton, and N. Dempster, *Mechano-chemical activation of high-Ca fly ash by cement free blending and gypsum aided grinding.* Construction and Building Materials, 2013. **43**: p. 480-489.
[58] Marku, J., I. Dumi, E. Lico, T. Dilo, and O. Cakaj, *The characterization and the utilization of cement kiln dust (CKD) as partial replacement of Portland cement in mortar and concrete production.* Zaštita materijala, 2012. **53**(4): p. 334-344.
[59] Siddique, R., *Utilization of cement kiln dust (CKD) in cement mortar and concrete—an overview.* Resources, conservation and recycling, 2006. **48**(4): p. 315-338.
[60] Attari, A., C. McNally, and M.G. Richardson, *A probabilistic assessment of the influence of age factor on the service life of concretes with limestone cement/GGBS binders.* Construction and Building Materials, 2016. **111**: p. 488-494.
[61] Limbachiya, V., E. Ganjian, and P. Claisse, *Strength, durability and leaching properties of concrete paving blocks incorporating GGBS and SF.* Construction and Building Materials, 2016. **113**: p. 273-279.
[62] Rahman, A.A., S. Abo-El-Enein, M. Aboul-Fetouh, and K. Shehata, *Characteristics of Portland blast-furnace slag cement containing cement kiln dust and active silica.* Arabian Journal of Chemistry, 2016. **9**: p. S138-S143.

[63] Jafer, H., W. Atherton, M. Sadique, F. Ruddock, and E. Loffill, *Stabilisation of soft soil using binary blending of high calcium fly ash and palm oil fuel ash.* Applied Clay Science, 2018. **152**: p. 323-332.
[64] Wild, S., J.M. Kinuthia, G.I. Jones, and D.D. Higgins, *Effects of partial substitution of lime with ground granulated blast furnace slag (GGBS) on the strength properties of lime-stabilised sulphate-bearing clay soils.* Engineering Geology, 1998. **51**: p. 37-53.
[65] Blanco, F., M.P. Garcia, J. Ayala, G. Mayoral, and M.A. Garcia, *The effect of mechanically and chemically activated fly ashes on mortar properties.* Fuel, 2006. **85**(14-15): p. 2018-2026.
[66] Al Hawesah, H., A. Shubbar, and R.L. Al Mufti. *Non-destructive assessment of early age mortar containing stainless steel powder*. in *The 17th Annual International Conference on Asphalt, Pavement Engineering and Infrastructure 21st -22nd February*. 2018. Liverpool, UK.
[67] Beushausen, H., M. Alexander, and Y. Ballim, *Early-age properties, strength development and heat of hydration of concrete containing various South African slags at different replacement ratios.* Construction and Building Materials, 2012. **29**: p. 533-540.
[68] Chaunsali, P. and S. Peethamparan, *Influence of the composition of cement kiln dust on its interaction with fly ash and slag.* Cement and Concrete Research, 2013. **54**: p. 106-113.
[69] Peethamparan, S., J. Olek, and J. Lovell, *Influence of chemical and physical characteristics of cement kiln dusts (CKDs) on their hydration behavior and potential suitability for soil stabilization.* Cement and concrete research, 2008. **38**(6): p. 803-815.
[70] Harbec, D., A. Tagnit-Hamou, and F. Gitzhofer, *Waste-glass fume synthesized using plasma spheroidization technology: Reactivity in cement pastes and mortars.* Construction and Building Materials, 2016. **107**: p. 272-286.
[71] Sadique, M. and H. Al-Nageim, *Hydration kinetics of a low carbon cementitious material produced by physico-chemical activation of high calcium fly ash.* Journal of Advanced Concrete Technology, 2012. **10**(8): p. 254-263.